

Dew amount and its long-term variation in the Kunes River Valley, Northwest China

FENG Ting^{1,2,3,4}, HUANG Farong^{1,2,4,5}, ZHU Shuzhen^{1,2,3,4}, BU Lingjie^{1,2,3,4}, QI Zhiming⁶, LI Lanhai^{1,2,3,4,5*}

¹ State Key Laboratory of Desert and Oasis Ecology, Xinjiang Institute of Ecology and Geography, Chinese Academy of Sciences, Urumqi 830011, China;

² Tianshan Station for Snowcover and Avalanche Research, Chinese Academy of Sciences, Xinyuan 835800, China;

³ University of Chinese Academy of Sciences, Beijing 100049, China;

⁴ Xinjiang Key Laboratory of Water Cycle and Utilization in Arid Zone, Urumqi 830011, China;

⁵ Research Center for Ecology and Environment of Central Asia, Chinese Academy of Sciences, Urumqi 830011, China;

⁶ Department of Bioresource Engineering, McGill University, Montreal H3A0G4, Canada

Abstract: Dew is an essential water resource for the survival and reproduction of organisms in arid and semi-arid regions. Yet estimating the dew amount and quantifying its long-term variation are challenging. In this study, we elucidate the dew amount and its long-term variation in the Kunes River Valley, Northwest China, based on the measured daily dew amount and reconstructed values (using meteorological data from 1980 to 2021), respectively. Four key results were found: (1) the daily mean dew amount was 0.05 mm during the observation period (4 July–12 August and 13 September–7 October of 2021). In 35 d of the observation period (i.e., 73% of the observation period), the daily dew amount exceeded the threshold ($>0.03 \text{ mm/d}$) for microorganisms; (2) air temperature, relative humidity, and wind speed had significant impacts on the daily dew amount based on the relationships between the measured dew amount and meteorological variables; (3) for estimating the daily dew amount, random forest (RF) model outperformed multiple linear regression (MLR) model given its larger R^2 and lower MAE and RMSE; and (4) the dew amount during June–October and in each month did not vary significantly from 1980 to the beginning of the 21st century. It then significantly decreased for about a decade, after it increased slightly from 2013 to 2021. For the whole meteorological period of 1980–2021, the dew amount decreased significantly during June–October and in July and September, and there was no significant variation in June, August, and October. Variation in the dew amount in the Kunes River Valley was mainly driven by relative humidity. This study illustrates that RF model can be used to reconstruct long-term variation in the dew amount, which provides valuable information for us to better understand the dew amount and its relationship with climate change.

Keywords: dew amount; long-term variation; meteorological variables; random forest model; multiple linear regression model; Kunes River Valley

Citation: FENG Ting, HUANG Farong, ZHU Shuzhen, BU Lingjie, QI Zhiming, LI Lanhai. 2022. Dew amount and its long-term variation in the Kunes River Valley, Northwest China. Journal of Arid Land, 14(7): 753–770. <https://doi.org/10.1007/s40333-022-0099-4>

1 Introduction

Dew is a vital source of freshwater that directly condenses from the nearby surrounding environment. As an important part of the Earth's water cycle, dew can be found in almost all

*Corresponding author: LI Lanhai (E-mail: lilh@ms.xjb.ac.cn)

Received 2022-04-27; revised 2022-06-13; accepted 2022-06-28

© Xinjiang Institute of Ecology and Geography, Chinese Academy of Sciences, Science Press and Springer-Verlag GmbH Germany, part of Springer Nature 2022

climate zones and ecosystems around the world (Gerlein-Safdi et al., 2018). Particularly, in the arid and semi-arid regions where water resources are scarce, dew is a proven essential water source (Tuure et al., 2019; Hill et al., 2020), whose hydrological and ecological effects are substantial. In arid and semi-arid regions, dewfall amount can account for more than 50% of rainfall amount, even exceeding the amount of rainfall in specific periods (Hao et al., 2012; Jia et al., 2019). Dew plays an important role in maintaining the water balance and it can efficiently reduce water loss caused by soil evaporation (Xiao et al., 2009; Meissner et al., 2010; Lekouch et al., 2011). Moreover, dew can alleviate water deficit in vegetation because leaves may directly absorb it (Vaadia and Waisel, 1963; Boucher et al., 1995; Zheng et al., 2011) and it can reduce the transpiration rates of plants (Munn é-Bosch et al., 1999). Therefore, dew can promote the growth of plants and increase their aboveground or belowground biomass (Boucher et al., 1995; Munn é-Bosch and Alegre, 1999; Jacobs et al., 2000; Zheng et al., 2011; Zhuang and Ratcliffe, 2012). Furthermore, dew is a crucial source of water for insects and small animals in desert environments (Steinberger et al., 1989), because they can sustain themselves by drinking dew directly or by eating hygroscopic vegetation that has absorbed dew (Hamilton and Seely, 1976; Broza, 1979). Accordingly, both the hydrological and ecological significance of dew cannot be neglected, particularly in the arid and semi-arid regions.

The major limitation in quantifying the function of dew is the difficulty of measurement, and there is yet no standard and worldwide method or instrument for dew measurement (Zangvil, 1996; Hao et al., 2012; Zhuang and Zhao, 2017). Since the last century, various dew-measuring devices have been developed, including the cloth-plate, plywood, glass-plate, and polyethylene-plate methods. These methods are collectively referred to as artificial-condensation surface methods to measure the dew amount (Kidron, 1998, 1999; Zhuang and Zhao, 2017; Tuure et al., 2019). Another method relies on microlysimeters (Jacobs et al., 1999; Richard, 2004; Meissner et al., 2007; Hao et al., 2012) to obtain the dew amount via direct weighing at the beginning and end of the condensation process (Zhuang and Zhao, 2017). However, both methods require manual operation every day during the measurement period. Consequently, it is difficult to obtain continuous and long-term data on the measured dew amount. More effective observation instruments, such as Open Path Eddy Covariance (OPEC) system and Bowen Ratio Energy Balance (BREB) system based on the energy-balance principle, have been applied to measure the dew amount (Kalthoff et al., 2006; Moro et al., 2007; Hao et al., 2012; Zhuang and Zhao, 2017), which can automatically measure the near-surface meteorological variables and energy flux. The difficulty of continuous measurement has been resolved by the advent of these advanced techniques. Nevertheless, prior to their emergence, historical continuous data on the dew amount is still unavailable.

Moreover, some researchers have developed physical models, semi-empirical models, and empirical models to simulate the dew condensation (Moro et al., 2007). Physical models generally view the dew condensation process as the inverse process of evaporation; hence, the negative latent heat flux can represent the dew condensation. For example, Jacobs et al. (2002, 2008) developed the models based on land surface-vegetation-soil energy balance to predict the potential dewfall and dew amount from an artificial dew collector. In addition, the single-source Penman-Monteith evaporation model has been applied to calculate the condensation of water vapor (Monteith, 1965; Jacobs et al., 2006; Moro et al., 2007; Uclés et al., 2013). Some other researchers have developed semi-empirical models with simple parameters or an empirical relationship in the physical models to simulate the dew condensation. For instance, in order to simulate the dew amount, Nikolayev et al. (1996) constructed a physical model based on the surface energy balance of dew condenser, which parameterized the emissivity of sky, emissivity of dew condenser, and absorptivity of short-wave radiation. Semi-empirical models and physical models have proven to be relatively accurate in dew estimation (Moro et al., 2007; Uclés et al., 2013), likely because they are based on the dew condensation mechanism and their model parameters have definite physical meanings, which can better reflect the energy transformation of the dew condensation process. However, there are still some uncertainties in these models, given

that they generally rely on a simplification of the condensation surface energy balance. Moreover, these models require input variables with fine temporal resolution (generally half-hour or hour), as dew generally forms at night, which hinders their applicability when only daily data is available. Empirical models, such as a statistical model or machine learning model, can fill this gap. For example, using a multiple linear regression (MLR) model, Hao et al. (2012) predicted the daily dew amount and its duration based on daily net radiation and actual vapor pressure. Furthermore, Lekouch et al. (2012) developed a model for the dew amount prediction based on artificial neural networks. Although empirical models are limited in characterizing the physical mechanism of dew, they are useful and practical when the time resolution of input variables is not sufficiently fine and there are too few of them, particularly for the reconstructions of long-term historical dataset of the dew amount.

Based on the methods above, researchers have made numerous observations and predictions of the dew condensation in arid and semi-arid regions. Zhuang and Zhao (2017) found that the most important factors affecting dew condensation are related to near-surface meteorological parameters. Temperature and water vapor conditions are considered as two critical parameters that control dew condensation (Beysens, 1995; Hao et al., 2012; Zhuang and Zhao, 2017). Low air and soil temperatures, high relative humidity, and moderate wind speed are known to be a favorable condition for dew condensation (Monteith, 1957; Zangvil, 1996). On the other hand, random forest (RF) model has proven to be an effective machine learning model in eco-hydrological variable reconstruction (Xu et al., 2018; Fu et al., 2021; Zhang et al., 2021). However, there are few studies using meteorological variables to reconstruct the dew condensation process over a long period with an RF model.

Arid and semi-arid regions in China account for 53% of its land area, and they are expanding yearly (Zhuang and Zhao, 2017). Studies of dew in China have mainly focused on these arid regions. For instance, Zhang et al. (2009) investigated the effects of three different types of biological soil crusts and bare sand on dew deposition in the Gurbantunggut Desert; dew condensation and its long-term trend in the Taklimakan Desert were elucidated by Hao et al. (2012); and dew's accumulation amount and duration were investigated in desert-oasis ecotone (Zhuang and Zhao, 2014, 2017). Most studies about dew conducted in arid and semi-arid regions of northwest China were conducted in extremely arid desert regions (Zhang et al., 2009; Hao et al., 2012; Zhuang and Zhao, 2014, 2017; Guo et al., 2022), leaving fewer that have analyzed or estimated the dew amount in semi-arid regions.

The Kunes River Valley, located in the upstream of the Ili River in northwest China, lies within a semi-arid region and is a key agricultural region (Liu et al., 2017a, 2020). Thus, investigating the dew amount and its long-term variation in the Kunes River Valley is imperative. Hence, the objectives of this study were to: (1) quantify the dew amount in summer and autumn using measurements from cloth-plate method; (2) reconstruct the long-term dew amount using RF and MLR models based on the relationships between the measured dew amount and meteorological variables; and (3) explore the long-term variation in the dew amount by utilizing the reconstructed values of RF model or MLR model and assess which model can better estimate the dew amount. These findings are pivotal for understanding the long-term dew condensation, and will assist in analyzing the effects of climate change on hydrological processes.

2 Materials and methods

2.1 Study area

This study was conducted in an observation field of Ili Station for Watershed Ecosystem Research (Ili Station), Chinese Academy of Science (43°20'N, 84°00'E; 1157 m a.s.l.), located in the Kunes River Valley in Northwest China (Fig. 1). The study area lies in a valley surrounded by mountains on three sides (Fig. 1a). The climate in this region is temperate continental, characterized mainly by semi-arid climate. The average annual precipitation in the valley ranges from 200 to 800 mm,

the average annual evaporation ranges from 1260 to 1900 mm (Liu et al., 2017b). The annual frost-free period is approximately 130–170 d and the average annual sunshine duration ranges from 2700 to 3000 h (Xu et al., 2011). Vegetation is mainly consisting of Gramineae, Leguminosae, Compositae, etc. The soil type is dominated by alpine meadow soil.

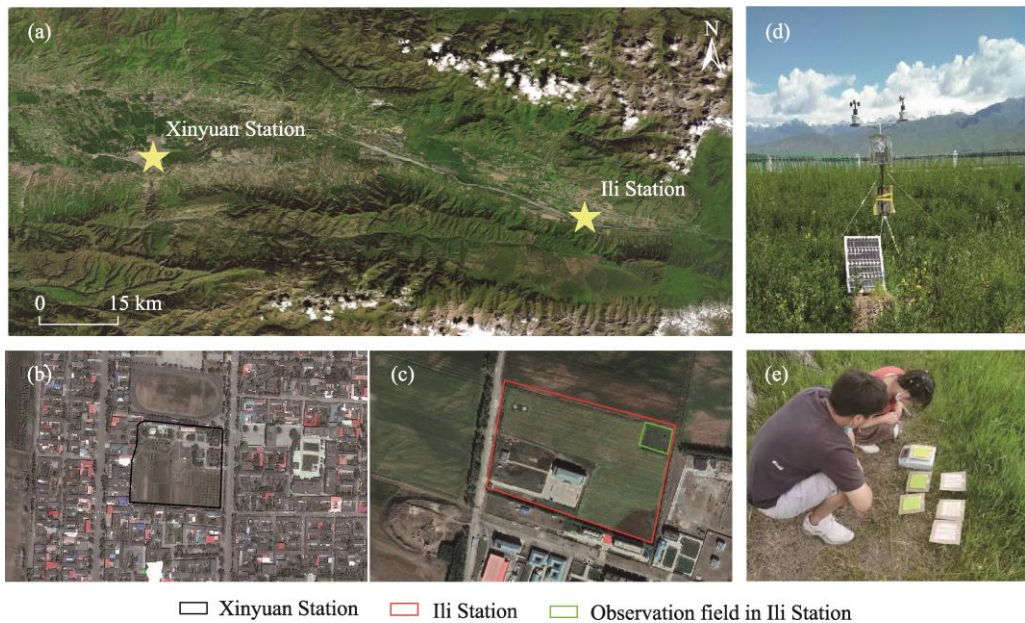


Fig. 1 Location of the study area (a); national weather station in Xinyuan County (Xinyuan Station, b); observation field in Ili Station for Watershed Ecosystem Research, Chinese Academy of Sciences (Ili Station, c); automatic weather station used in this study (d); and measurement of the daily dew amount based on the cloth-plate method in observation filed (e).

2.2 Experimental design and data collection

2.2.1 Dew amount measurement

The daily dew amount was measured in summer (from 4 July to 12 August) and autumn (from 13 September to 7 October) of 2021. The daily dew amount was collected and measured by the cloth-plate method (Kidron, 1988; Zhuang and Zhao, 2014). Cloth patches (each 10.00 cm×10.00 cm×0.15 cm) were attached to the center of three glass plates (each 15.00 cm×15.00 cm×0.20 cm) overlaid on a piece of plywood (15.00 cm×15.00 cm×0.20 cm) to create an isolated and homogenous substratum (Kidron, 1988). The measured dew amount was calculated as the difference in weight before and after dew collection (Fig. 1e). Specifically, the clean and dry cloth-plate devices were weighed and placed in the observation field of Ili Station at 20:00 (LST) the day prior to measurement. At 6:00 the next morning before sunrise, each cloth-plate device was individually weighed, and the differences in weights were designated as the dew production for that night. The dew amount (Dew_{amount} ; mm) was calculated as follows:

$$Dew_{amount} = \frac{10 \times (W_r - W_s)}{S}, \quad (1)$$

where W_r is the weight of cloth-plate device before sunrise (g); W_s is the weight of the cloth-plate device after sunset (g); and S is the surface area of a cloth patch (cm^2).

2.2.2 Meteorological data

Meteorological variables used to analyze their bivariate correlations with the measured dew amount were measured by an automatic weather station (Fig. 1d), located at the observation field of Ili Station (Fig. 1c). These measured meteorological variables included air temperature, relative humidity, wind speed, net solar radiation, atmospheric pressure, soil moisture at 10 cm depth, soil temperature at 10 cm depth, and soil surface temperature. These data were obtained at a frequency

of 10 Hz and recorded every 5 min by a CR1000 data logger (Campbell scientific Inc., Logan, Utah, United States); they were stored as 30-min average values. Based on the 30-min average values, we can get the daily values (including mean, minimum, and maximum) and nocturnal values (including mean, minimum, and maximum) by resampling.

Given that the Ili Station was established after 2010, meteorological data used to reconstruct the long-time series of the dew amount were collected from the nearest national weather station in Xinyuan County (Xinyuan Station) and its data archive of long-term continuously observed meteorological data (Fig. 1a and 1b). The Xinyuan Station and Ili Station are both located within the Kunes River Valley, and their meteorological conditions are similar. Thus, meteorological data from Xinyuan Station can generally convey the regional meteorological conditions at the study site. Considering that the dew amount observation period spanned early July to early October in 2021, we chose the nearly half-year (i.e., from June 2021 to October 2021) time scale with similar environmental conditions to that in the observed period to estimate the long-term variation in the dew amount from 1980 to 2021. The long-term meteorological data used in this study included daily minimum air temperature, daily mean relative humidity, daily mean wind speed, daily precipitation, and monthly precipitation.

2.3 Reconstruction of the dew amount based on multiple linear regression (MLR) model and random forest (RF) model

In this study, we applied MLR and RF models to reconstruct the dew amount using Python 3.8. The MLR model is expressed as follows:

$$y = a_1x_1 + a_2x_2 + \dots + a_nx_n + b, \quad (2)$$

where y is the daily dew amount (mm/d); x_1, x_2, \dots, x_n are the meteorological variables explaining the variation in the daily dew amount on a corresponding date; a_1, a_2, \dots, a_n are regression coefficients of x_1, x_2, \dots, x_n , respectively; and b is the intercept. The predictors selected for the fitting of the dew amount depended on the relationships between the measured dew amount and meteorological variables (i.e., daily minimum temperature, daily mean temperature, daily maximum temperature, daily mean relative humidity, daily mean wind speed, daily mean soil moisture at 10 cm depth, daily mean soil temperature at 10 cm depth, and daily mean net solar radiation).

The predictors used in RF model were the same as those in MLR model. In this study, we used a grid search algorithm (Lujan-Moreno et al., 2018) to explore the optimal parameter combination for fitting the dew amount according to RF model. The feature importance of each predictor obtained via RF model was ranked. Note that feature importance refers to the contribution rate of each predictor to the overall fitting accuracy; hence, the sum of the feature importance of all predictors for an RF model is 100%, that is the larger the feature importance, the more important the predictor.

2.4 Statistical analysis

2.4.1 Relationship between the measured dew amount and meteorological variables

Pearson correlation coefficient was used to test the relationship between the measured dew amount and each meteorological variable. Considering the mechanism of dew condensation is complex, we used the non-parametric Mann-Whitney U test to identify the significant influence of meteorological variables on the dew amount. Namely, we determined the significant difference of a given meteorological variable between the nights with large dew amount (>0.10 mm) and the nights with small dew amount (<0.03 mm) at 95% confidence level.

2.4.2 Evaluation of model performance

The determination coefficient (R^2), mean absolute error (MAE), and root mean square error (RMSE) were used to evaluate the goodness-of-fit of each MLR and RF model. The MAE and RMSE were calculated as follows:

$$\text{MAE} = \frac{1}{m} \sum_{i=1}^m |h(x_i) - y_i|, \quad (3)$$

$$\text{RMSE} = \sqrt{\frac{1}{m} \sum_{i=1}^m (h(x_i) - y_i)^2}, \quad (4)$$

where MAE is the mean absolute error (mm/d); RMSE is the root mean square error (mm/d); m is the sample capacity; $h(x_i)$ is the predicted value; and y_i is the measured value.

2.4.3 Variation in reconstructed trend for dew amount

We applied two methods to analyze the variation in the reconstructed dew amount from 1980 to 2021. First, the Sen's slope estimator (β) was used to obtain the annual variation magnitude in the dew amount (Theil, 1950; Sen, 1968); a value of β greater than 0.00 represents an increasing trend, whereas a value of β less than 0.00 represents a decreasing trend. Then, because this method lacks statistical significance testing for the variation trend, we utilized the Mann-Kendall (MK) test to analyze the significance of the variation trend (Mann, 1945; Kendall, 1975). Based on the absolute Z value of the test statistic from the MK test, if $|Z|$ is greater than 1.96, the trend is significant at 5% level. According to the values of β and $|Z|$, we divided the variation in the dew amount into five categories: significantly increase ($\beta > 0.00$ and $|Z| > 1.96$), significantly decrease ($\beta < 0.00$ and $|Z| > 1.96$), increase ($\beta > 0.00$ and $|Z| \leq 1.96$), decrease ($\beta < 0.00$ and $|Z| \leq 1.96$), and no obvious variation (Huang et al., 2021).

3 Results

3.1 Measured dew amount and its relationship with meteorological variables

In this study, the dew amount was measured from 4 July to 12 August and from 13 September to 7 October in 2021 to represent the measured dew amount in summer and autumn, respectively. The precondition for the dew condensation is that the temperature of condensation surface is lower than or equal to the dew point temperature. Figure 2 showed the nocturnal mean dew point temperature and nocturnal mean soil surface temperature during measurement period. Evidently, the nocturnal mean soil surface temperature was almost higher than the nocturnal mean dew point temperature. In addition, soil moisture at 10 cm depth declined at night (Fig. 2b).

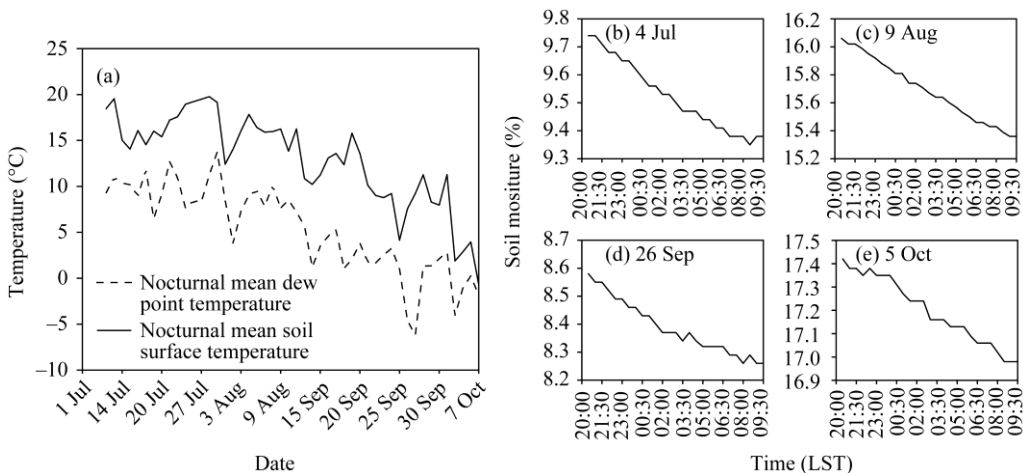


Fig. 2 Nocturnal mean dew point temperature and nocturnal mean soil surface temperature (a) and soil moisture at 10 cm depth on 4 July (b), 9 August (c), 26 September (d), and 5 October (e) in 2021

Combining these results with the criteria of dew types reported by previous study, it can be concluded that the measured dew amount corresponds to the total canopy condensation. Therefore, the main dew type in the Kunes River Valley arises from canopy condensation, and

this study thus focuses on this dew type.

The observation period included 48 d with the dew amount measurement and 15 d with precipitation at night (measurement could not be conducted as precipitation occurred at night). Total recorded of the dew amount was 2.50 mm, with a daily mean value of 0.05 mm (Fig. 3). As can be seen from Figure 3, the dew amount in autumn was relatively higher than that in summer. The daily mean dew amount in summer and autumn was 0.04 and 0.06 mm, respectively, and the total dew amount in summer and autumn was 1.12 and 1.46 mm, respectively. Previous study demonstrated that 0.03 mm was the threshold amount of dew availability for microorganisms. We found that the daily dew amount greater than 0.03 mm occurred on 35 d, accounting for 73% of the total measurement days.

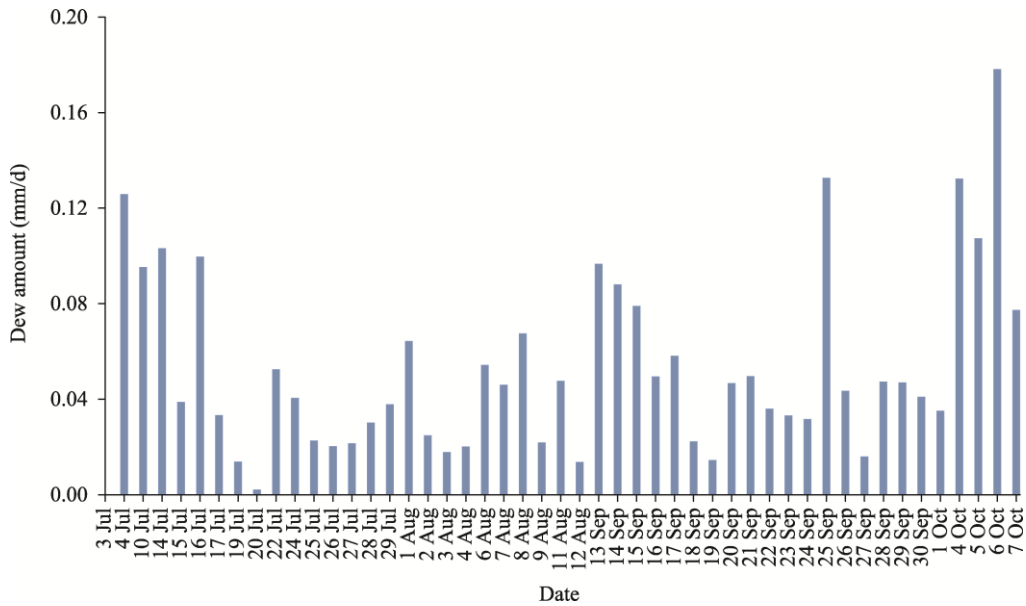


Fig. 3 Measured dew amount based on the cloth-plate method in summer and autumn of 2021

The dew amount is often closely related to meteorological conditions. In order to further understand the relationship between meteorological variables and the dew amount, we analyzed correlations between them at a daily scale. The result showed that air temperature (including daily minimum air temperature, daily mean air temperature, and daily maximum air temperature), soil temperature at 10 cm depth, and net solar radiation exhibited negative correlations with the dew amount, whereas positive correlations were found for daily mean relative humidity, daily mean wind speed, and soil moisture at 10 cm depth (Fig. 4). However, only the temperature variables and relative humidity were significantly ($P<0.05$) correlated with the dew amount, being stronger for the former than the latter. Correlations between the dew amount and other variables (daily mean wind speed, soil moisture at 10 cm depth, and net solar radiation) were not statistically significant ($P>0.05$).

Previous studies have shown that the influence of wind speed, net solar radiation, and soil moisture on the dew amount should not be ignored. Thus, we analyzed the significance of differences in meteorological variables of nights with the dew amount more than 0.10 mm and those with the dew amount less than 0.03 mm based on the non-parametric Mann-Whitney U test. The result was presented in Table 1. Nights with the dew amount more than 0.10 mm exhibited lower wind speed, higher relative humidity, and lower temperatures than nights with the dew amount less than 0.03 mm, and these differences were significant ($P<0.001$; Table 1). By contrast, no significant differences ($P>0.001$) were detected in soil moisture of nights with the dew amount more than 0.10 mm and soil moisture of nights with the dew amount less than 0.03 mm. It was clear that low temperature, high relative humidity, and low wind speed are

conducive to the dew condensation.

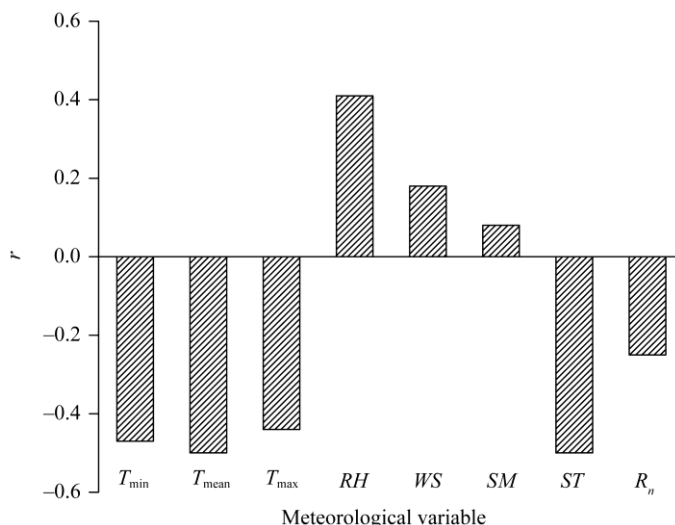


Fig. 4 Correlation coefficient (r) between the dew amount and meteorological variables. T_{\min} , daily minimum air temperature; T_{mean} , daily mean air temperature; T_{\max} , daily maximum air temperature; RH , daily mean relative humidity; WS , daily mean wind speed; SM , soil moisture at 10 cm depth; ST , soil temperature at 10 cm depth; R_n , net solar radiation.

Table 1 Meteorological variables of nights with the dew amount more than 0.10 mm and those with the dew amount less than 0.03 mm in the study site

| Meteorological variables | | Nights with the dew amount more than 0.10 mm | Nights with the dew amount less than 0.10 mm | Significance level |
|---|---------|--|--|--------------------|
| Air temperature (°C) | Minimum | 1.50 | 9.80 | <0.001 |
| | Maximum | 30.40 | 33.90 | |
| | Mean | 9.27 | 17.23 | |
| Relative humidity (%) | Minimum | 36.60 | 25.10 | <0.001 |
| | Maximum | 80.10 | 65.40 | |
| | Mean | 64.24 | 45.45 | |
| Wind speed (m/s) | Minimum | 0.00 | 0.00 | <0.001 |
| | Maximum | 4.57 | 5.58 | |
| | Mean | 1.22 | 1.52 | |
| Soil moisture at 10 cm depth (%) | Minimum | 8.26 | 8.29 | 0.034 |
| | Maximum | 17.85 | 25.84 | |
| | Mean | 13.32 | 13.69 | |
| Soil temperature at 10 cm depth (°C) | Minimum | 9.10 | 13.56 | <0.001 |
| | Maximum | 21.76 | 23.66 | |
| | Mean | 14.25 | 19.40 | |
| Net solar radiation (W/m ²) | Minimum | -105.05 | -107.48 | 0.366 |
| | Maximum | 220.70 | 207.20 | |
| | Mean | -55.98 | -55.26 | |

Note: Significance was determined at the 95% confidence level by a non-parametric Mann-Whitney U test.

According to the above results, we found that the main meteorological variables affecting the daily dew amount were air temperature, relative humidity, wind speed, and soil temperature at 10 cm depth ($P<0.001$). Given that the daily minimum air temperature generally occurred at night

when dew formed and soil temperature data was unavailable during the long-term period, we used the daily minimum air temperature, daily mean relative humidity, and daily mean wind speed to simulate the daily dew amount during 1980–2021 based on the MLR and RF models.

3.2 Performance of the daily dew amount fitting models

This subsection presents the performance of MLR and RF models for the daily dew amount simulation. MLR and RF models were trained with 50% of the measured dew amount data and then tested with the other 50%, respectively. The two models used the same training and testing dataset that were randomly distinguished in Python 3.8. The values of R^2 , RMSE, and MAE for the testing dataset are shown in Figure 5.

Compared with MLR model, the performance of RF model was better by virtue of its larger R^2 and smaller RMSE and MAE (Fig. 5). The R^2 of RF model reached 0.55 ($P<0.05$), and its RMSE and MAE were only 0.031 and 0.024 mm/d, respectively; while, the R^2 of MLR model was 0.34, with RMSE and MAE being 0.037 and 0.027 mm/d, respectively. Compared with MLR model, the total dew amount (1.25 mm) and the daily mean dew amount (0.05 mm) estimated by RF model were closer to the measured total dew amount (1.34 mm) and the measured daily mean dew amount (0.06 mm).

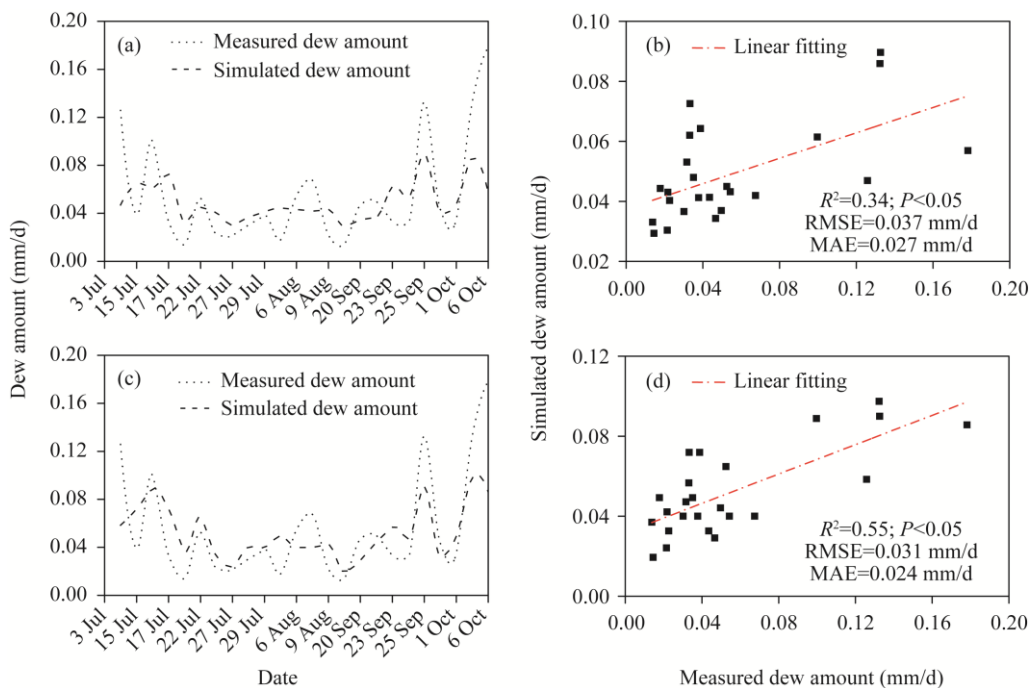


Fig. 5 Performance of multiple linear regression (MLR) and random forest (RF) models on the dew amount simulation. (a) and (c), the measured and simulated dew amount based on MLR and RF models, respectively; (b) and (d), the relationship of the measured dew amount with the dew amount simulated by MLR model and the dew amount simulated by RF model, respectively; RMSE, root mean square error; MAE, mean absolute error.

To compare the simulation performance of MLR and RF models in detail, we classified the dew amount into five intervals, including 0.00–0.03, 0.03–0.05, 0.05–0.10, 0.10–0.15, and 0.15–0.20 mm, and then drew the frequency distribution histograms of the measured and simulated daily dew amount (Fig. 6). Both MLR and RF models showed deviations in the simulated dew amount. Notable, both models underestimated the dew amount in the low-value (0.00–0.03 mm) and high-value (0.10–0.20 mm) intervals. Particularly, for the interval of 0.10–0.20 mm, neither model yielded the dew amount. Moreover, the two models overestimated the dew amount in the range of 0.03–0.10 mm. For the testing dataset, although there were deviations in the dew amount simulated by the two models, compared with MLR, the frequency

of the dew amount simulated by RF model was generally closer to the frequency of the measured dew amount.

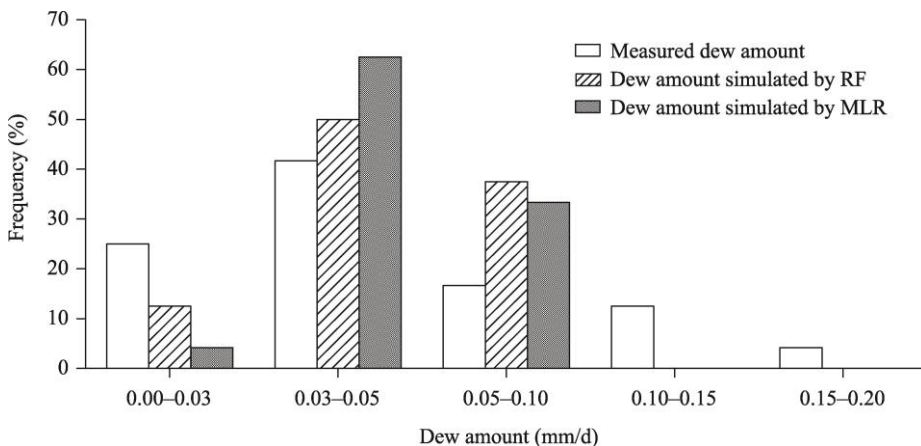


Fig. 6 Frequency distribution histograms of the dew amount for the testing dataset

Consistent with the above results in this section, RF model performed better than MLR model in the daily dew amount simulation, in terms of R^2 , RMSE, MAE, and frequency distribution. Therefore, we choose RF model to simulate the long-term variation in the dew amount in the Kunes River Valley.

3.3 Long-term variation in the dew amount

Evaluating long-term variation in the dew amount is difficult due to the lack of long-term direct observations. Here, we used a RF model to assess the long-term variation in the dew amount based on the conventional meteorological observation data. To avoid the errors caused by precipitation, we deleted the data containing precipitation in the statistics and results.

3.3.1 Statistics for the monthly dew amount

Figure 7 showed the simulated monthly dew amount during June–October from 1980 to 2021, as well as the daily mean, maximum, and minimum dew amount of each month. The monthly dew amount ranged from 0.33 (June 2013) to 1.91 mm (October 1980). The dew amount in most (80%) months exceeded the threshold amount of dew availability for microorganisms (0.90 mm).

There was no obvious difference in the monthly dew amount among different months, except for October. The mean dew amount in October (1.35 mm) surpassed that in other months, being the lowest in June (Fig. 8). The monthly dew amount was 1.09, 1.10, and 1.12 mm in August, September, and July, respectively.

3.3.2 Variation in the dew amount

We analyzed the long-term variation in the dew amount during June–October and in each month (Fig. 9; Table 2). Besides the entire study period (from 1980 to 2021), we divided the dew amount series during June–October and in each month into three temporal stages, namely, Stage 1 (from 1980 to 2002), Stage 2 (from 2002 to 2013), and Stage 3 (from 2013 to 2012), according to the maximum and minimum dew amount during June–October from 1980 to 2021.

The results from the Sen's slope and MK test showed that the dew amount during June–October was characterized by a significantly decreasing trend from 1980 to 2021 ($\beta < 0.00$ and $|Z| > 1.96$), as well as the dew amount in July and September showed a significantly decreasing trend. However, their variation rates (i.e., absolute value of β) were all less than 0.02 per year. The dew amount in other months showed no obvious variation trend from 1980 to 2021 ($|Z| < 1.96$).

Variation in the dew amount differed among the different temporal stages. Namely, the dew amount during June–October and in each month decreased significantly in Stage 2 (Fig. 9). In this stage, the declined trend during June–October was the highest ($\beta = -0.31$), but the variation rate in

each month was always lower than 0.10. However, in Stage 1 and Stage 3, the variation trends of the dew amount during June–October and in each month were all insignificant ($|Z|<1.96$). Further, the dew amount variation showed no obvious trend ($\beta=0.00$) in July or October in Stage 1; while, in the other months, it was distinguished by an increasing trend ($\beta>0.00$; $|Z|<1.96$). Moreover, the variation in the dew amount featured an increasing trend in Stage 3 during June–October and in each month, exceeding that in Stage 1.

It was concluded that the dew amount during June–October and in each month slightly increased or did not change significantly from 1980 to 2002, but then sharply decreased until 2013, and finally displayed a slightly increasing trend from 2013 to 2021 (Fig. 9). Moreover, the dew amount during June–October decreased significantly from 1980 to 2021 (Table 2).

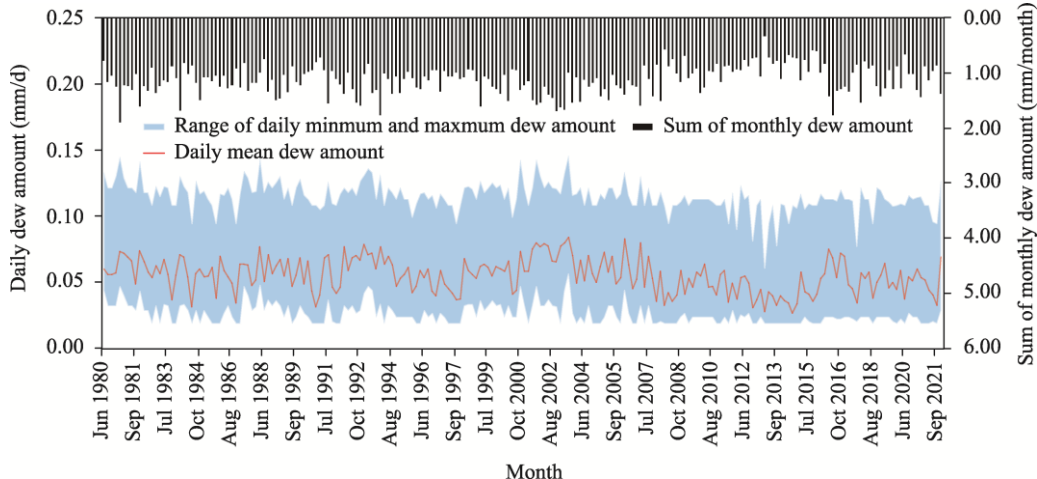


Fig. 7 Simulated monthly dew amount and the daily mean, maximum, and minimum dew amount during June–October from 1980 to 2021

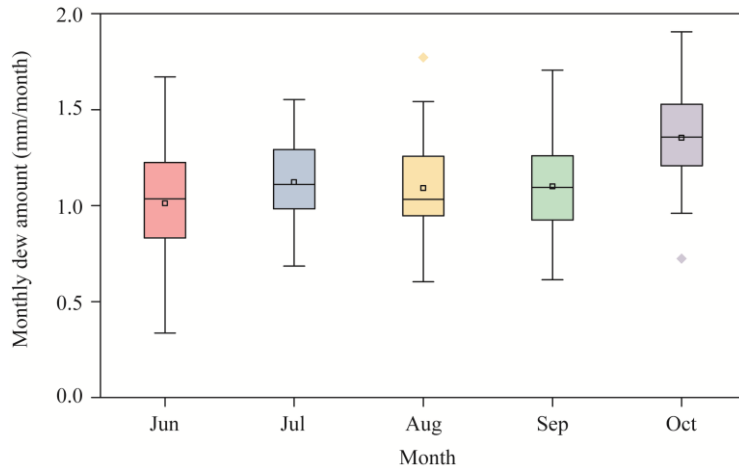


Fig. 8 Boxplot for the monthly dew amount during June–October from 1980 to 2021. The boxes represent the range from the lower quantile (Q25) to the upper quantile (Q75) of the total monthly dew amount during June–October from 1980 to 2021. The dots and horizontal lines inside the boxes represent the means and medians, respectively. The dots outside the boxes represent outliers. The upper and lower whiskers indicate the maximum and minimum values, respectively.

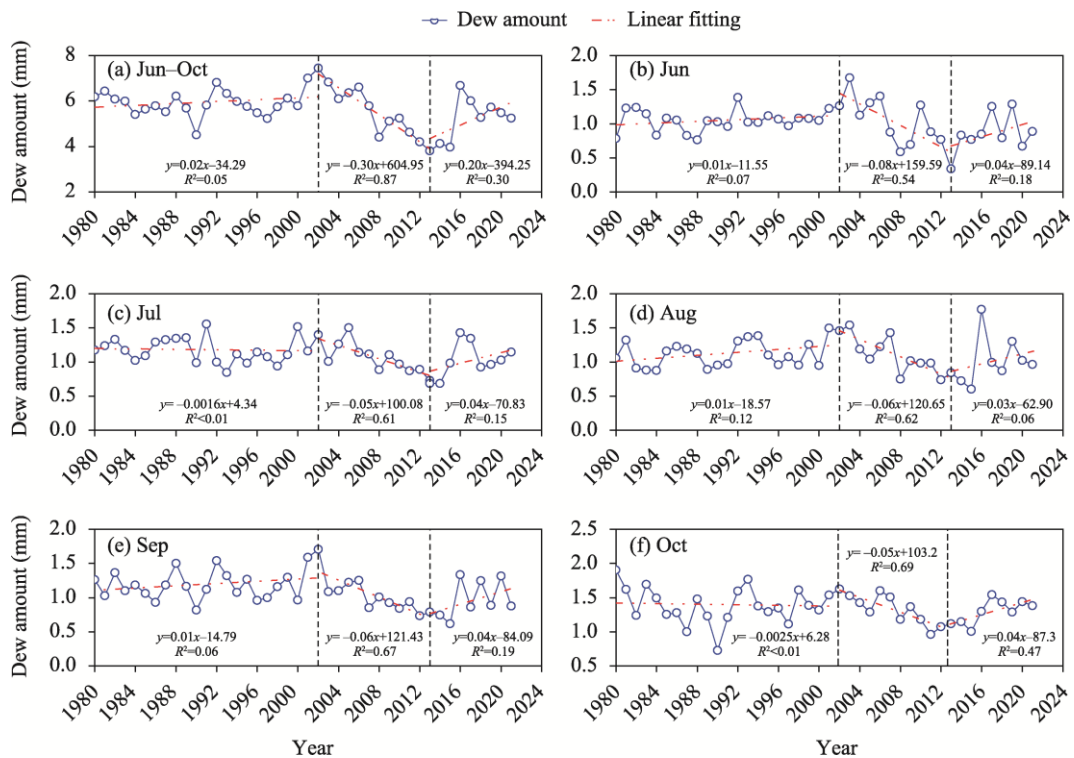


Fig. 9 Variation in the dew amount during June–October (a) and in June (b), July (c), August (d), September (e), and October (f) from 1980 to 2021

4 Discussion

Manual measurements of the dew amount were carried out in the Kunes River Valley in summer and autumn of 2021, providing valuable information about the dew condensation dynamics. Based on the empirical data, we trained and applied RF model to estimate the long-term dew amount. This is an important attempt to simulate the historical trend of the dew amount for 42 a (1980–2021) based on a machine learning model.

4.1 Measured dew amount and its correlation with meteorological variables

This work started with the dew amount observations. Specifically, in order to measure the dew amount, we used the cloth-plate method (Kidron, 1998), a method previously used to robustly measure the dew amount in the Negev Desert in south Israel (Kidron, 1998; Kidron et al., 2002; Kidron, 2005), as well as the Badain Jaran Desert in northwestern China (Zhuang and Zhao, 2014). The results of our study showed that the daily dew amount was concentrated in 0.03–0.10 mm (its frequency was 60%) during the observation period. Our results are generally consistent with findings reported for the Badain Jaran Desert (Zhuang and Zhao, 2014; Zhuang et al., 2021). Manual measurement of the dew amount provided us with valuable information about daily dew condensation, by analyzing the relationship between the dew amount and meteorological variables. Previous studies found that dew condensation is a complex physical process, influenced by numerous micrometeorological variables (Ye et al., 2007; Wang and Zhang, 2011; Hao et al., 2012). He and Richards (2015) reported that clear skies, moderate winds, strong inversions of temperature from the ground surface to the atmosphere, low surface temperatures, and high relative humidity were all favorable abiotic conditions for water vapor condensation. Our results showed that air temperature, relative humidity, and wind speed have robust relationships with the dew amount, which is similar to previous studies. Moreover, Zhuang and Zhao (2017) reported

Table 2 Long-term variation in the dew amount in different temporal stages

| Month | Temporal stage | β | $ Z $ | Trend |
|--------------|----------------|---------|-------|------------------------|
| June–October | 1980–2002 | 0.01 | 0.32 | Increase |
| | 2002–2013 | -0.31 | 3.50 | Significantly decrease |
| | 2013–2021 | 0.20 | 0.73 | Increase |
| | 1980–2021 | -0.02 | 2.08 | Significantly decrease |
| June | 1980–2002 | 0.01 | 0.85 | Increase |
| | 2002–2013 | -0.08 | 2.13 | Significantly decrease |
| | 2013–2021 | 0.02 | 1.15 | Increase |
| | 1980–2021 | 0.00 | 0.98 | No obvious variation |
| July | 1980–2002 | 0.00 | 0.26 | No obvious variation |
| | 2002–2013 | -0.05 | 2.95 | Significantly decrease |
| | 2013–2021 | 0.05 | 1.15 | Increase |
| | 1980–2021 | -0.01 | 2.10 | Significantly decrease |
| August | 1980–2002 | 0.01 | 1.43 | Increase |
| | 2002–2013 | -0.06 | 2.95 | Significantly decrease |
| | 2013–2021 | 0.03 | 0.94 | Increase |
| | 1980–2021 | 0.00 | 0.80 | No obvious variation |
| September | 1980–2002 | 0.01 | 0.69 | Increase |
| | 2002–2013 | -0.05 | 2.81 | Significantly decrease |
| | 2013–2021 | 0.02 | 1.15 | Increase |
| | 1980–2021 | -0.01 | 2.36 | Significantly decrease |
| October | 1980–2002 | 0.00 | 0.00 | No obvious variation |
| | 2002–2013 | -0.05 | 2.95 | Significantly decrease |
| | 2013–2021 | 0.04 | 1.56 | Increase |
| | 1980–2021 | 0.00 | 1.26 | No obvious variation |

that high relative humidity was a prerequisite for water vapor condensation, and that 50% was the lowest value of relative humidity enabling dew condensation. In addition, dew is controlled by wind speed and how wind speed affects dew condensation is complex (Zhuang and Zhao, 2017).

This might explain why we did not find a significant correlation between the dew amount and wind speed ($P>0.05$), not unlike that reported by Hao et al. (2012). However, in our study, there was a significant difference in wind speed at night when the dew amount was greater than 0.10 mm and less than 0.03 mm. Mean wind speed and maximum wind speed at night with the dew amount greater than 0.10 mm were 1.22 and 4.57 m/s, respectively, corresponding to moderate wind speed. This finding supports other work showing that moderate wind speed can enhance the transport of water vapor and prevent the mixing of air at the ground surface with air above it (He and Richards, 2015). Previous studies also indicated that high wind speed inhibits the dew condensation (Monteith, 1957; Nilsson, 1996; Lekouch et al., 2012; Zhuang and Zhao, 2017), but this study cannot reflect this opinion.

4.2 Estimation of the dew amount

A physical model to estimate the dew amount is not easy to set-up because the detailed thermal and radiative exchange of condensation surface cannot be accurately modeled. An alternative is to predict the dew amount based on the empirical relationship between the condensation volume and meteorological variables (Lekouch et al., 2012). Traditional statistical model, such as MLR

model, may be successfully used to predict the dew amount based on the correlation between it and meteorological variables (Hao et al., 2012). Because machine learning model is an efficient and robust mathematical technique of non-linear regression, which includes various capabilities, such as classification and prediction (Zhang et al., 1998), it can be implemented to estimate the dew amount from meteorological data. Machine learning model, for instance, an artificial neural network, has been applied to predict the dew point temperature (Shank et al., 2008) and the dew amount (Lekouch et al., 2012). Here, we selected daily minimum air temperature, daily mean relative humidity, and daily mean wind speed as predictors to construct MLR and RF models to simulate the daily dew amount, and we compared the performance between RF model and MLR model. It is clear that RF model captured the dew amount variability better than MLR model, with smaller MAE and RMSE as well as higher R^2 . The R^2 of RF model increased by 62% compared with MLR model, and correspondingly reduced the MAE and RMSE by 14% and 19%, respectively. This improvement was mainly attributed to the strong adaptability of RF model, which could detect and express the non-linear relationships between the dew amount and meteorological variables. This advantage of RF model can also be illustrated by the results for its feature importance values.

4.3 Long-term variation in the dew amount and its driven factors

In this study, we developed RF model to derive the long-term variation in the dew amount from 1980 to 2021. During the period, the most special period is from 2002 to 2013, when the dew amount significantly declined for about a decade. Using MLR model, Hao et al. (2012) reported a similar significantly decreasing trend of the dew amount over the same years in the Taklimakan Desert, near our study area, but they did not try to explain the decreasing trend. To that end, we analyzed the variation in daily minimum air temperature, daily mean relative humidity, and daily mean wind speed, and total precipitation during June–October from 1980 to 2021 (Fig. 10).

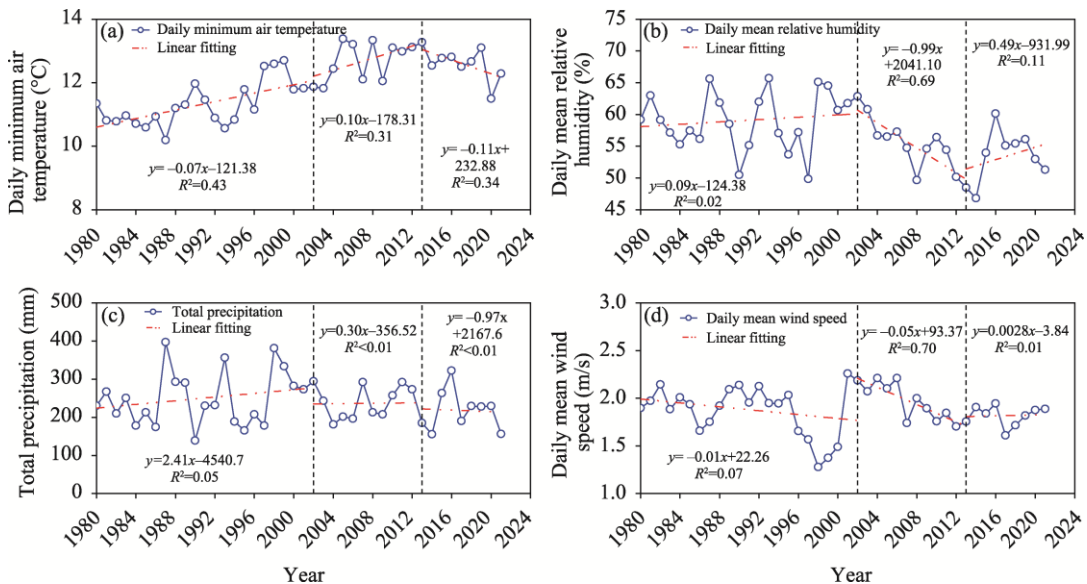


Fig. 10 Variation in daily minimum air temperature (a), daily mean relative humidity (b), total precipitation (c), and daily mean wind speed (d) during June–October from 1980 to 2021

During the past 42 a, the variation in daily mean relative humidity showed a similar pattern to the change of the dew amount. As shown in Figure 10, daily mean relative humidity significantly decreased from 2002 to 2013, implying that the difficulty of attaining saturation for water vapor in the air, and this directly led to the reduction of the dew amount. Still, the reduction in daily mean relative humidity might have arisen from the increase of daily minimum air temperature and precipitation. Evidently, the daily minimum air temperature kept increasing from 2002 to 2013.

Although higher air temperature enables more water vapor stored in the atmosphere (Allen et al., 1998), the precipitation was almost stable, which suggests the overall source of atmospheric moisture might vary negligibly. As a result, there was a decrease in daily mean relative humidity.

4.4 Limitations of this study

The current study has some limitations, mainly concerning the measurement and estimation of the dew amount. First, we chose the cloth-plate method to empirically measure the dew amount in the field. This method has the advantages of practicality and low cost. But like other artificial condensation surface methods, their obtained results are often influenced by the compositions of the artificial surface (Jacobs et al., 2008; Hao et al., 2012; Zhuang and Zhao, 2017). Moreover, the cloth-plate method cannot accurately reflect the physical mechanism of dew condensation process that would occur on a natural condensation surface, though it still has climatological relevance to some extent. To better understand natural dew condensation mechanism, future researches should focus on observing and comparing natural condensation surface. The long-term dew amount estimated by RF and MLR model can reflect the climatological significance of the dew amount from 1980 to 2021, since we trained and fitted RF and MLR in the same way based on the relationship between the measured dew amount by the cloth-plate method and meteorological variables. However, as empirical-based methods, MLR and RF models cannot reflect the energy transformation of dew condensation process like the physical models based on energy balance, such as the Penman-Monteith evaporation model. Second, it is more informative to compare the performance of MLR and RF models with other approaches, such as the Penman-Monteith model, with empirical parameters used for the estimation of the dew amount. The Penman-Monteith model needs data with high temporal resolution to estimate the dew amount, while the lack of that data in available long-term datasets impairs their usage in deriving long-term variations in the dew amount data based on Penman-Monteith model. As main aim of this study was to obtain a long-term series of the dew amount data, we relied on MLR and RF models because they only required data at a daily scale to estimate the dew amount. In the future, we will consider comparing the performance of MLR and RF models with that of Penman-Monteith and other physical models for the estimation of the dew amount.

The large-scale weighing lysimeter is currently a relatively perfect tool for measuring the dew amount, which can measure the dew amount on the land surface simply and reliably. The future researches on land surface dewfall should try to combine different methods, namely, the large-scale weighing lysimeter, Open Path Eddy Covariance (OPEC) system, Bowen Ratio Energy Balance (BREB) system, measurement of common meteorological variables with high temporal resolution, and numerical models based on the physical mechanism of dew condensation.

5 Conclusions

Evaluating long-term variations in the dew amount is difficult due to the lack of long-term direct observation and the limitations of relevant estimation methods. To explore the long-term variation in the dew amount in the Kunes River Valley, we compared the performance of MLR and RF models in the dew amount simulation. We selected the predictors used in MLR and RF models based on the relationship between meteorological variables and the measured daily dew amount in summer and autumn of 2021. It is concluded that dew formed frequently in the study area, where the daily dew amount exceeded the threshold amount of dew availability for microorganisms in most (73%) of dew-measured days. The mean daily dew amount in autumn was a little higher than that in summer. Air temperature, relative humidity, and wind speed played important roles in dew condensation; the threshold for dew condensation was relative humidity greater than 60% and wind speed less than 1.5 m/s. In addition, RF model generally performed better than MLR model, resulting a higher value of R^2 and lower MAE and RMSE for the dew amount estimation. According to the dew amount reconstructed by RF during June–October from 1980 to 2021, we found that the dew amount in most months (80%) exceeded the threshold amount of dew availability for

microorganisms. There were differences in the variations of dew amount among different temporal stages from 1980 to 2021. The dew amount during June–October slightly increased before the beginning of the 21st century, then it fell significant for about a decade, and rebounded slightly from 2013 to 2021. Long-term variation in the dew amount was primarily impacted by relative humidity.

The present study is of great significance to explore the characteristic of the historical dew amount. The findings could help to explore how climate change affects dew condensation, and further to maintain the ecology stability in arid and semi-arid regions under the background of climate change.

Acknowledgements

This work was supported by the National Natural Science Foundation of China (41901048), the Project of State Key Laboratory of Desert and Oasis Ecology, Xinjiang Institute of Ecology and Geography, Chinese Academy of Sciences (E151030101), the Project of National Cryosphere Desert Data Center of China (2021kf02), and the Youth Innovation Promotion Association of the Chinese Academy of Sciences (2021438). We are grateful for the fieldwork support from members of the Ili Station for Watershed Ecosystem Research, Chinese Academy of Sciences.

References

Allen R G, Pereira L S, Raes D, et al. 1998. Crop evapotranspiration: guidelines for computing crop water requirements. Fao Irrigation and Drainage Paper 56. Rome: Food and Agriculture Organization of the United Nations.

Beysens D. 1995. The formation of dew. *Atmospheric Research*, 39(1–3): 215–237.

Boucher J F, Munson A D, Bernier P Y. 1995. Foliar absorption of dew influences shoot water potential and root growth in *Pinus strobus* seedlings. *Tree Physiology*, 15(12): 819–823.

Broza M. 1979. Dew, fog and hygroscopic food as a source of water for desert arthropods. *Journal of Arid Environments*, 2(1): 43–49.

Fu T L, Li X R, Jia R L, et al. 2021. A novel integrated method based on a machine learning model for estimating evapotranspiration in dryland. *Journal of Hydrology*, 603: 126881, doi: 10.1016/j.jhydrol.2021.126881.

Gerlein-Safdi C, Koohafkan M C, Chung M, et al. 2018. Dew deposition suppresses transpiration and carbon uptake in leaves. *Agricultural and Forest Meteorology*, 259: 305–316.

Guo X N, Wang Y F, Yan H M, et al. 2022. Dew/hoar frost on the canopies and underlying surfaces of two typical desert shrubs in Northwest China and their relevance to drought. *Journal of Hydrology*, 609: 127880, doi: 10.1016/j.jhydrol.2022.127880.

Hamilton W J, Seely M K. 1976. Fog basking by the Namib Desert beetle, *Onymacris unguicularis*. *Nature*, 262(5566): 284–285.

Hao X M, Li C, Guo B, et al. 2012. Dew formation and its long-term trend in a desert riparian forest ecosystem on the eastern edge of the Taklimakan Desert in China. *Journal of Hydrology*, 472: 90–98.

He S Y, Richards K. 2015. The role of dew in the monsoon season assessed via stable isotopes in an alpine meadow in Northern Tibet. *Atmospheric Research*, 151: 101–109.

Hill A J, Lincoln N K, Rachmilevitch S, et al. 2020. Modified hiltner dew balance to re-estimate dewfall accumulation as a reliable water source in the Negev Desert. *Water*, 12(10): 2952, doi: 10.3390/w12102952.

Huang F R, Feng T, Guo Z K, et al. 2021. Impact of winter snowfall on vegetation greenness in Central Asia. *Remote Sensing*, 13(21): 4205, doi: 10.3390/rs13214205.

Jacobs A F G, Heusinkveld B G, Berkowicz S M. 1999. Dew deposition and drying in a desert system: a simple simulation model. *Journal of Arid Environments*, 42(3): 211–222.

Jacobs A F G, Heusinkveld B G, Berkowicz S M. 2002. A simple model for potential dewfall in an arid region. *Atmospheric Research*, 64(1–4): 285–295.

Jacobs A F G, Heusinkveld B G, Kruit R J W, et al. 2006. Contribution of dew to the water budget of a grassland area in the Netherlands. *Water Resources Research*, 42(3): W03415, doi: 10.1029/2005wr004055.

Jacobs A F G, Heusinkveld B G, Berkowicz S M. 2008. Passive dew collection in a grassland area, The Netherlands. *Atmospheric Research*, 87(3–4): 377–385.

Jia Z F, Ma Y D, Liu P, et al. 2019. Relationship between sand dew and plant leaf dew and its significance in irrigation water

supplementation in Guanzhong Basin, China. *Environmental Earth Sciences*, 78(12): 354, doi: 10.1007/s12665-019-8345-6.

Kalthoff N, Fiebig-Wittmaack M, Meißner C, et al. 2006. The energy balance, evapo-transpiration and nocturnal dew deposition of an arid valley in the Andes. *Journal of Arid Environments*, 65(3): 420–443.

Kendall M G. 1975. *Rank Correlation Methods*. London: Charles Griffin.

Kidron G J. 1998. A simple weighing method for dew and fog measurements. *Weather*, 53(12): 428–433.

Kidron G J. 1999. Differential water distribution over dune slopes as affected by slope position and microbiotic crust, Negev Desert, Israel. *Hydrological Processes*, 13(11): 1665–1682.

Kidron G J. 2005. Angle and aspect dependent dew and fog precipitation in the Negev desert. *Journal of Hydrology*, 301(1–4): 66–74.

Lekouch I, Muselli M, Kabbachi B, et al. 2011. Dew, fog, and rain as supplementary sources of water in south-western Morocco. *Energy*, 36(4): 2257–2265.

Lekouch I, Lekouch K, Muselli M, et al. 2012. Rooftop dew, fog and rain collection in southwest Morocco and predictive dew modeling using neural networks. *Journal of Hydrology*, 448: 60–72.

Liu X, Ma J, Ma Z W, et al. 2017a. Soil nutrient contents and stoichiometry as affected by land-use in an agro-pastoral region of northwest China. *CATENA*, 150: 146–153.

Liu X, Li L H, Qi Z M, et al. 2017b. Land-use impacts on profile distribution of labile and recalcitrant carbon in the Ili River Valley, northwest China. *Science of the Total Environment*, 586: 1038–1045.

Liu X, Chen D T, Yang T, et al. 2020. Changes in soil labile and recalcitrant carbon pools after land-use change in a semi-arid agro-pastoral ecotone in Central Asia. *Ecological Indicators*, 110: 105925, doi: 10.1016/j.ecolind.2019.105925.

Lujan-Moreno G A, Howard P R, Rojas O G, et al. 2018. Design of experiments and response surface methodology to tune machine learning hyperparameters, with a random forest case-study. *Expert Systems with Applications*, 109: 195–205.

Madeira A C, Kim K S, Taylor S E, et al. 2002. A simple cloud-based energy balance model to estimate dew. *Agricultural and Forest Meteorology*, 111(1): 55–63.

Mann H B. 1945. Nonparametric tests against trend. *Econometrica*, 13(3): 245–259.

Meissner R, Seeger J, Rupp H, et al. 2007. Measurement of dew, fog, and rime with a high-precision gravitation lysimeter. *Journal of Plant Nutrition and Soil Science*, 170(3): 335–344.

Meissner R, Rupp H, Weller U, et al. 2010. Lysimeter research in Europe—technological developments and research strategies. In: 19th World Congress of Soil Science: Soil Solutions for a Changing World. Brisbane, Australia.

Monteith J L. 1957. Dew. *Quarterly Journal of the Royal Meteorological Society*, 83(357): 322–341.

Moro M J, Were A, Villagarcía L, et al. 2007. Dew measurement by Eddy covariance and wetness sensor in a semiarid ecosystem of SE Spain. *Journal of Hydrology*, 335(3–4): 295–302.

Munné-Bosch S, Alegre L. 1999. Role of dew on the recovery of water-stressed *Melissa officinalis* L. plants. *Journal of Plant Physiology*, 154(5–6): 759–766.

Munné-Bosch S, Nogués S, Alegre L. 1999. Diurnal variations of photosynthesis and dew absorption by leaves in two evergreen shrub communities in Mediterranean field conditions. *New Phytologist*, 144(1): 109–119.

Nikolayev V S, Beysens D, Gioda A, et al. 1996. Water recovery from dew. *Journal of hydrology*, 182(1–4): 19–35.

Nilsson T. 1996. Initial experiments on dew collection in Sweden and Tanzania. *Solar Energy Materials and Solar Cells*, 40(1): 23–32.

Richards K. 2004. Observation and simulation of dew in rural and urban environments. *Progress in Physical Geography: Earth and Environment*, 28(1): 76–94.

Sen P K. 1968. Estimates of the regression coefficient based on Kendall's Tau. *Journal of the American Statistical Association*, 63: 1379–1389.

Steinberger Y, Loboda I, Garner W. 1989. The influence of autumn dewfall on spatial and temporal distribution of nematodes in the desert ecosystem. *Journal of Arid Environments*, 16(2): 177–183.

Theil H. 1950. A rank invariant method of linear and polynomial regression analysis: Part III. *Proceedings of the Royal Netherlands Academy of Sciences*, 53: 1397–1412.

Tuure J, Korpela A, Hautala M, et al. 2019. Comparison of surface foil materials and dew collectors location in an arid area: a one-year field experiment in Kenya. *Agricultural and Forest Meteorology*, 276–277: 107613, doi: 10.1016/j.agrformet.2019.06.012.

Uclés O, Villagarcía L, Moro M J, et al. 2013. Role of dewfall in the water balance of a semiarid coastal steppe ecosystem. *Hydrological Processes*, 28(4): 2271–2280.

Vaadia Y, Waisel Y. 1963. Water absorption by the aerial organs of plants. *Physiologia Plantarum*, 16(1): 44–51.

Xiao H, Meissner R, Seeger J, et al. 2009. Effect of vegetation type and growth stage on dewfall, determined with high precision weighing lysimeters at a site in northern Germany. *Journal of Hydrology*, 377(1–2): 43–49.

Xu T R, Guo Z X, Liu S M, et al. 2018. Evaluating different machine learning methods for upscaling evapotranspiration from flux towers to the regional scale. *Journal of Geophysical Research: Atmospheres*, 123(16): 8674–8690.

Xu Y J, Chen Y, Li W, et al. 2011. Distribution pattern of plant species diversity in the mountainous Region of Ili River Valley, Xinjiang. *Environmental Monitoring and Assessment*, 177(1): 681–694.

Zangvil A. 1996. Six years of dew observations in the Negev Desert, Israel. *Journal of Arid Environments*, 32(4): 361–371.

Zhang C, Luo G P, Hellwich O, et al. 2021. A framework for estimating actual evapotranspiration at weather stations without flux observations by combining data from MODIS and flux towers through a machine learning approach. *Journal of Hydrology*, 603: 127047, doi: 10.1016/j.jhydrol.2021.127047.

Zhang J, Zhang Y M, Downing A, et al. 2009. The influence of biological soil crusts on dew deposition in Gurbantunggut Desert, Northwestern China. *Journal of Hydrology*, 379(3–4): 220–228.

Zheng X J, Li S, Li Y. 2011. Leaf water uptake strategy of desert plants in the Junggar Basin, China. *Chinese Journal of Plant Ecology*, 35(9): 893–905. (in Chinese)

Zhuang Y L, Ratcliffe S. 2012. Relationship between dew presence and Bassia dasypylla plant growth. *Journal of Arid Land*, 4(1): 11–18.

Zhuang Y L, Zhao W Z. 2013. Dew variability in three habitats of a sand dune transect in a desert oasis ecotone, Northwestern China. *Hydrological Processes*, 28(3): 1399–1408.

Zhuang Y L, Zhao W Z. 2017. Dew formation and its variation in Haloxylon ammodendron plantations at the edge of a desert oasis, northwestern China. *Agricultural and Forest Meteorology*, 247: 541–550.

Zhuang Y L, Zhao W Z, Luo L H, et al. 2021. Dew formation characteristics in the gravel desert ecosystem and its ecological roles on Reaumuria soongorica. *Journal of Hydrology*, 603: 126932, doi: 10.1016/j.jhydrol.2021.126932.